

Collaboration Between RSK-EphA2 and Gas6-Axl RTK Signaling in Arginine Starvation Response That Confers Resistance to EGFR Inhibitors



Macus Tien Kuo^{*}, Yan Long^{*}, Wen-Bin Tsai^{*}, Ying-Ying Li^{†,‡}, Helen H.W. Chen[§], Lynn G. Feun[‡] and Niramol Savaraj^{†,‡,¶}

^{*}Department of Translational Molecular Pathology, The University of Texas MD Anderson Cancer Center, Houston, TX, USA; [†]Department of Medicine, University of Miami Miller School of Medicine, Miami, FL, USA; [‡]Sylvester Comprehensive Cancer Center, University of Miami Miller School of Medicine, Miami, FL, USA; [§]Department of Radiation Oncology, National Cheng Kung University Hospital, College of Medicine, National Cheng Kung University, Tainan, 70428, Taiwan; [¶]Division of Hematology and Oncology, Miami Veterans Affairs Healthcare System, Miami, FL, USA

Abstract

Many human malignancies require extracellular arginine (Arg) for survival because the key enzyme for *de novo* Arg biosynthesis, argininosuccinate synthetase 1 (ASS1), is silenced. Recombinant arginine deiminase (ADI-PEG20), which digests extracellular Arg, has been in clinical trials for treating ASS1-negative tumors. Reactivation of ASS1 is responsible for the treatment failure. We previously demonstrated that ASS1 reactivation is transcriptionally regulated by c-Myc via the upstream Gas6-Axl tyrosine kinase (RTK) signal. Here, we report that another RTK EphA2 is coactivated via PI3K-ERK/RSK1 pathway in a ligand-independent mechanism. EphA2 is also regulated by c-Myc. Moreover, we found that knockdown Axl upregulates EphA2 expression, demonstrating cross-talk between these RTKs. ADI^R cell lines exhibits enhanced sensitivities to nutrient deprivation such as charcoal-stripped FBS and multiple RTK inhibitor foretinib but resistance to EGFR inhibitors. Knockdown EphA2, and to lesser extent, Axl, overcomes EGFRi resistance. c-Myc inhibitor JQ1 can also sensitize ADI^R cells to ADI-PEG20. This study elucidates molecular interactions of multiple RTKs in Arg-stress response and offers approaches for developing strategies of overcoming ADI-PEG20 resistance.

Translational Oncology (2020) 13, 355–364

Introduction

Arginine (Arg) is required for supporting the highly proliferative activities in malignant cells. While Arg is a nonessential amino acid and can be obtained from extracellular source through cationic amino acid transporters including CAT-1 and CAT2B [1], Arg can also be *de novo* synthesized via the rate-limiting enzyme argininosuccinate synthetase 1 (ASS1) using citrulline and aspartate as substrates. It has been reported that a vast amount of tumors from different origins are ASS1-negative or expressed at very low levels. These include melanoma and hepatocellular carcinoma (HCC) (100%) [2], acute myeloid leukemia [3], prostate cancer, breast cancers, and lung cancers (55–90%) [4]. These tumors depend on extracellular Arg

Address all correspondence to: Niramol Savaraj, Department of Medicine, University of Miami Miller School of Medicine, Miami, FL, USA. E-mail: nsavaraj@med.miami.edu or Macus Tien Kuo, PhD, Department of Translational Molecular Pathology, The University of Texas MD Anderson Cancer Center, Houston, TX, USA. E-mail: tienkuo@sbcglobal.net
Received 3 June 2019; Revised 1 December 2019; Accepted 1 December 2019

Published by Elsevier Inc. on behalf of Neoplasia Press, Inc. This is an open access article under the CC BY-NC-ND license (<http://creativecommons.org/licenses/by-nc-nd/4.0/>).
1936-5233/19
<https://doi.org/10.1016/j.tranon.2019.12.003>

supply for survival. When the extracellular Arg source is depleted, these tumors die of Arg starvation by autophagy, leading to apoptosis [4,5].

Targeted Arg starvation therapy of ASS1-auxotrophic tumors, using Arg-degrading pegylated recombinant enzyme ADI-PEG20 (hereafter ADI will be used) which digests Arg into citrulline and ammonia, has been in several ongoing clinical investigations of different malignancies including acute myeloid leukemia [6], pancreatic adenocarcinoma [7], HCC [8], thoracic tumors [9], pleural mesothelioma [10], malignant melanoma [11], and advanced malignant solid tumors [12]. Another Arg-degrading recombinant protein, human arginase (rhArg or BCT-100) which digests Arg into ornithine and urea, has been in clinical investigations for treating acute lymphoblastic leukemia and HCC [13,14]. Recent phase II clinical studies showed that while ADI treatments rapidly deplete Arg levels in the circulation, however, Arg levels soon return to the basal levels [6,15]. Re-expression of ASS1 compromises the effectiveness of ADI therapy [16]. Thus, understanding ASS1 reactivation mechanism is of great importance for improving targeted Arg starvation therapy.

Early study demonstrated that ASS1 silencing in Arg-auxotrophic tumors is associated with epigenetic DNA methylation [17]. We have previously demonstrated that ASS1 silencing is due to transcriptional suppression by the negative transcriptional factor HIF1 α which binds the E-Box located at the ASS1 promoter [16]. Arg starvation rapidly induces chromatin remodeling complex P300-HDAC2-Sin3A which epigenetically deacetylates H3K14ac and H3K27ac at the ASS1 promoter. Following the PHD2-driven HIF1 α -degrading system, the promoter-bound HIF-1 α is degraded [18]. This allows c-Myc, which is also an E-Box binder, to turn on the expression of ASS1. Arg starvation rapidly triggers externalization of Gas6 to interact with its receptor tyrosine kinase (RTK) Axl via a reactive oxygen species (ROS)-related mechanism. This activates the downstream Ras-PI3 kinase-AKT-GSK3 β pathway, resulting in stabilization of c-Myc [19]. Elevated c-Myc can transcriptionally upregulate itself and also feed back to upregulate Axl, thereby amplifying the Arg-auxotrophic signaling [18,20]. Thus, Arg starvation stress response involves complexed epigenetic and genetic coupling feedback and feedforward mechanisms that control cellular Arg homeostasis (Figure 7).

Axl is a member of the TAM (Tyro3-Axl-TK-Mer) subfamily in the RTK family [21]. Axl plays important roles in tumor cell survival, proliferation, and progression and is frequently overexpressed in a variety of cancers [22,23]. Many recent studies have demonstrated that Axl is involved in epithelial-mesenchymal transition (EMT) that promotes cancer cell adhesion and metastasis and chemoresistance [24–28]. The EMT signaling involves a diverse spectrum of transcriptional regulatory networks [29] in that reprogram many important cellular processes including cancer metabolism such as glucose and glutamine dependence in ADI-resistant Axl-overproducing cells [30] and rewiring of the RTK signaling [25]. There are 58 known RTKs in humans sharing similar protein structures including extracellular ligand-binding domains and intracellular tyrosine kinase domains [31,32], but diverse mechanisms of activation and cell signaling [33]. Many RTKs even cross-talk to each other for performing concerted functions.

To better understand the roles of RTK family in Arg starvation response, we report here the identification of several RTKs that are sporadically upregulated in ADI-resistant (ADI^R) cell lines. Importantly, we found that EphA2 is consistently upregulated in the ADI^R cell lines tested. We characterized the mechanisms underlying EphA2

upregulation and its interaction with Axl in response to Arg stress. We further demonstrate that elevated EphA2 is involved in the development of resistance to EGFR inhibitors in the ADI^R cells. Our results provide mechanistic basis for developing improved treatment strategies in targeted Arg-deprivation cancer therapy.

Materials and Methods

Reagents, Antibodies, and siRNAs

Reagents were obtained from the following sources: ADI-PEG20 (specific activity, 5–10 IU/mg) from Polaris Pharmaceuticals Inc. (San Diego, CA); sulforhodamine B (SRB), Ly294002 from Sigma–Aldrich (St. Louis, MO); perifosine, PLX4720 and foretinib (XL880 or GSK1363089) from Selleck Lab (Houston, TX); PI-103 from Echelon Biosciences (Salt Lake City, UT); gefitinib and lapatinib from LC laboratories (Woburn, MA); JQ1 from AdooQ Bioscience (Irvine, CA).

Antibodies were obtained from the following sources: rabbit antibodies for hEGFR, p-EGFR, p-Axl, EphA2(ser897), and EphA2(Y588) from Cell Signaling (Danvers, MA); rabbit anti-Axl, p-Axl, EGFR, P-EGFR, hErbB2, p-hErbB2, HGF-1R, hIGF, EphA1, and α -tubulin antibodies were from R&D Laboratories (Minneapolis, MN). Polyclonal antiphosphotyrosine (p-Tyr) antibody from Thermo Fisher (Grand Island, NY); rabbit anti-EphA2 antibody from Bethyl laboratory (Houston, TX); anti-ASS1 antibody from Polaries.

Small interfering RNA (siRNA) for c-Myc and AXL has been published [20]; EphA2 (Cat. No. SASI_Hs01-00222676 and SASI-Hs01-000265), RSK (SASI_Hs01-00070213 and SASI_Hs02-00305126) were all obtained from Sigma-Aldrich (St. Louis, MD).

Cell Culture, siRNA Transfection, and SRB Cytotoxicity Assay

A2058 melanoma cells were purchased from the American Type Culture Collection Center (ATCC) cells and were maintained in Dulbecco's modified Eagle's medium (DMEM) containing 10% fetal bovine serum (FBS) at 5% CO₂ atmosphere. Independent ADI^R cell lines were developed by selecting surviving A2058 cells by continuously treated with stepwise increasing concentrations of ADI from 0.1 μ g/ml to 0.9 μ g/ml for 6 months as described previously [30]. Charcoal-stripped FBS was purchased from Life Technology (St Louis, MD). For Arg-depletion experiments, cells were maintained in the regular medium containing 0.3 μ g/mL of ADI for the lengths of time as indicated. In some experiments, cells were cultured in Arg-free DMEM containing 10% dialyzed FBS (Life Science Technology). All transfections were performed using Lipofectamine 2000 (Invitrogen, St Louis, MD) in accordance with manufacturer's instructions. For the cytotoxicity assay, cells were seeded in 96-well plates (4 \times 10³ cells per well) and cultured with different concentrations of inhibitors with or without ADI for 72 hours. Cells were fixed with 50% trichloroacetic acid followed by staining with 0.4% SRB in 1% acetic acid for 30 min at room temperature. Plates were washed five times with 1% acetic acid to remove unbound dye. Bound dye was dissolved by adding 10 mM unbuffered Tris base. Cell proliferation was calculated by measuring optical density (OD) at 564 nm using a spectrophotometer.

Phospho-RTK Array Analysis

The Human Phospho-RTK Array Kit from R&D Systems was used to determine the relative levels of tyrosine phosphorylation of 42

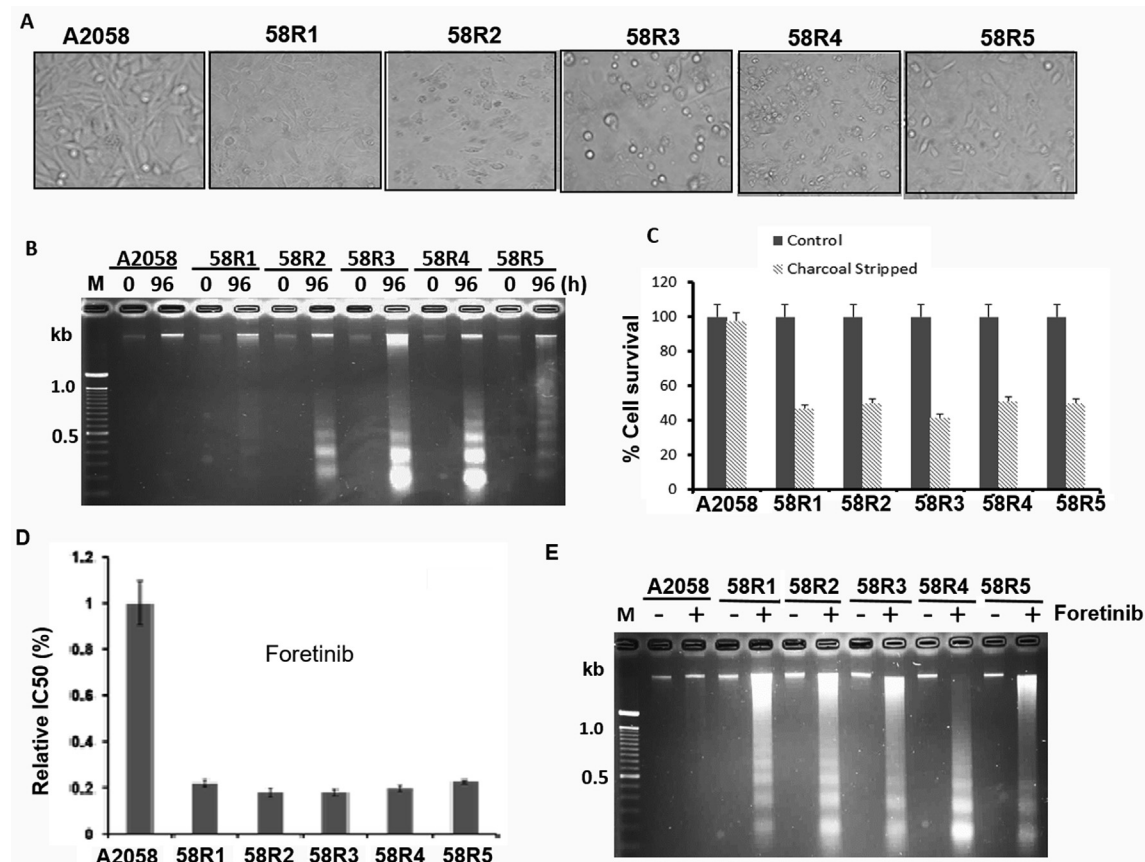


Figure 1. ADI^R cells are sensitive to nutrient stress and RTK inhibitor foretinib. (A) Phase-contrast morphology of five ADI^R cells (58R1 to 58R5) and ADI-sensitive cells (A2058) cultured in medium containing charcoal-stripped FBS for 96 hours; (B) and (C) proliferation measurements of cells cultured under charcoal-stripped FBS for 96 hours by DNA fragmentation and by SRB assays, respectively; (D) and (E) cell proliferation measurements of A2058 and ADI^R cells treated with foretinib (2 nM, 48 hours) and determined by SRB assay and by DNA fragment assay, respectively. RTK, receptor tyrosine kinase; SRB, sulforhodamine B.

distinct RTKs, in accordance with the manufacturer's protocol. The arrays were incubated with 500 μ g of protein lysates prepared from cells with or without ADI treatment overnight at 4 °C. The arrays were washed and incubated with a horseradish peroxidase-conjugated phospho-tyrosine detection antibody (1:5000 dilution) and visualized using an enhanced chemiluminescence kit (Thermo Scientific).

Other Procedures

Procedures for preparation of cell extracts, Western blotting [18,19], and apoptosis analysis using DNA fragmentation were described previously [16,19]. All Western blotting procedures were performed at least two times, and results were reproducible using actin and/or α -tubulin as control. Only representative images were presented. Statistical analysis was performed by Student t-test using Microsoft Excel 2007 program. A *P* value < 0.05 was regarded as significant. Error bars represent the standard error of the mean (SEM).

Results

ADI-Resistant Cells Exhibit Elevated Sensitivities to Serum Deprivation in Culture

We previously established nine independent ADI^R cell clones from two melanoma cell lines, five from A2058 cells (designated as 58R1 to

58R5) and four from SK-mel-2. All these cell lines have the same mechanism of ADI resistance, *i.e.*, elevated ASS1 express and metabolic abnormalities, *i.e.*, elevated glycolytic (Warburg effect) and glutaminolytic activities as compared with their parental cells [30]. In this study, we used the A2058 ADI^R series for investigations. Because glucose-derived carbon and glutamine-derived nitrogen metabolites are essential for cultured cell survival, proliferation, and stress resistance [34], we hypothesized that ADI^R variants may be more vulnerable to general nutritional deprivation than do their parental counterpart. To test this hypothesis, we cultured the parental cell line (A2058) and its five independently established ADI^R lines in serum-free medium for 96 hours. By phase-contrast microscopy which is a simple and reliable method for detecting apoptotic cells [35], we found that ADI^R cells show shrinkage morphology and detachment from the neighboring cells, membrane blebbing, and formation of apoptotic bodies, characteristics of apoptotic cells, whereas the parental cells mostly remain morphologically intact (Figure 1A). Induction of apoptosis in ADI^R cell lines by serum starvation determined by DNA fragmentation assay is shown in Figure 1B and by measuring cell proliferation activity using SRB [36] in Figure 1C.

Using charcoal-stripped FBS to remove substantial amounts of growth factors and hormones [37], we previously showed that all these ADI^R variants exhibited enhanced PI3K-AKT axis [30], a downstream of RTK signaling. These results suggest that activation of

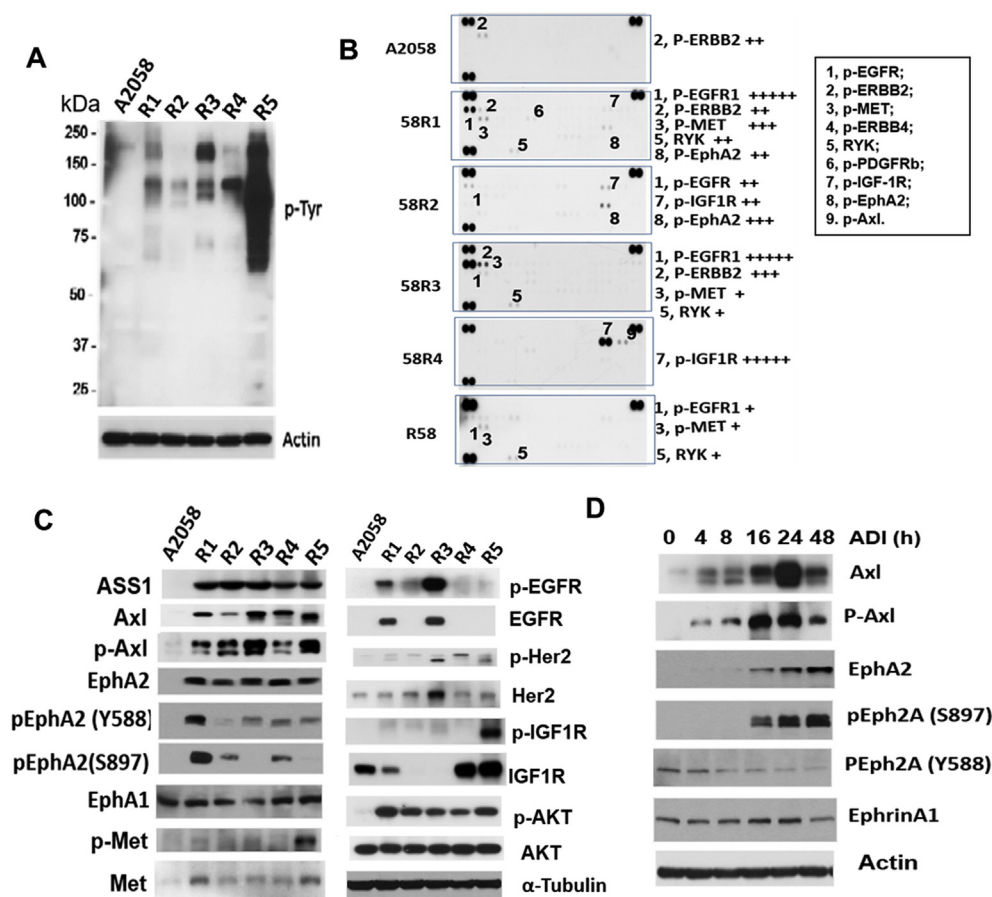


Figure 2. Analyses of RTK expression in ADI^R cells. (A) Western blots of ADI^R and A2058 cell lysates using anti-phosphorylated Tyr antibody; (B) determination of activation of various RTKs by phosphor-RTK array; (C) Western blots showing elevated expression of ASS1 and various RTK in A2058 and in five ADI^R cells; (D) time-dependent activation of Axl and EphA2 in A2058 cells treated with ADI (0.5 μg/ml) for the time as indicated. RTK, receptor tyrosine kinase.

RTK may be involved in these ADI^R cells [38]. Consistent with this context, we found that in comparison with the parental cells, all five A2058 ADI^R variants are more sensitive to the killing by foretinib, an ATP-competitive multiple RTKs inhibitor [39], using SRB cell proliferation (Figure 1D) and DNA fragmentation/apoptosis assays (Figure 1E).

Enhanced Expression of Multiple RTKs in the ADI^R Cells

Activation of RTKs involves protein phosphorylation, most frequently at the tyrosine residues (Tyr). We performed Western blotting to probe p-Tyr levels in ADI^R cells. Figure 2A shows the results of a Western blot, indicating that p-Tyr levels in all the five ADI^R cells are higher than in the A2058 cells.

To identify which RTKs are activated in the ADI^R cells, we prepared lysates from five ADI^R and the A2058 cells to probe an array of 42 different anti-RTK antibodies in duplicate immobilized on a membrane. We found that many different RTKs were elevated in different ADI^R cell lines and that levels of activation were varied among these ADI^R cells (Figure 2B and Table 1). This assay uses total cell lysates as probes, and it is convenient for initial survey of RTK expression, but results need to be substantiated using additional methods. We therefore performed Western blotting using individual anti-RTK antibodies to probe the cell lysates. We observed that all these ADI^R cell lines show elevated expression of p-Axl and Axl, and

p-AKT and ASS1, consistent with the characters of ADI^R cells as described [20] (Figure 2C). Moreover, we found that EphA2 and Met levels are elevated in all five A2058 ADI^R cell lines, whereas levels of EGFR/pEGFR, Her2/pHer2, and IGF1R/pIGF1R are elevated in some but not all ADI^R cell lines.

In this study, we focused on EphA2 investigation because it is overexpressed in all 5 clones. Using site-specific anti-p-EphA2 antibodies in Western blotting, we demonstrated that elevated EphA2 in ADI^R cells are phosphorylated either at the tyrosine Y588 and/or at the serine S897 residues. Interestingly, levels of Ephrin A1, which is the ligand of EphA2, were not elevated in these ADI^R cells as compared with that in the A2058 cell line. It has been reported that EphA2(Y588) phosphorylation is mainly ligand-dependent, whereas EphA2(S897) phosphorylation is ligand-independent [40,41].

Table 1. Quantitative results of phospho-RTK array analysis in parental and ADI^R A2058 cell lines

	A2058	58R1	58R2	58R3	58R4	58R5
p-EGFR1		+++++	++	+++++		+
p-ERBB2	++	++		+++		
P-MET		+++		+		+
p-ERBB4						
RYK		++		+		+
p-PDGFRb						
p-IGF-1R			++		+++++	
p-EphA2		++	+++			

These ADI^R cells were established by long-term exposure of A2058 cells to ADI [30]. To investigate the short-term effects on EphA2 expression by ADI, we treated A2058 cells with 0.5 μg/ml of ADI from 4 to 48 hours. We found that while induction of Axl/p-Axl occurs within 4 hours after the treatment, significant induction of EphA2 and p-EphA2(S897) occurs 16 hours after the treatment (Figure 2D). In contrast, levels of p-EphA2(Y588) decreased as treatment time increased, whereas Ephrin A1 level remained with no change. These results indicate that the ligand-independent induction of EphA2 phosphorylation occurs early during ADI^R development.

The PI3K-RSK Signal is Involved in the Upregulation of EphA2 By ADI

Previous studies have demonstrated that phosphorylation of EphA2(S897) is regulated by the p90 ribosomal S6 kinase (RSK) via the MET/EKT/AKT pathway [42–44]. To investigate whether this pathway is involved in ADI-induced EphA2 induction, we treated A2058 cells with ADI for different lengths of time. We found that while the steady-state RSK-1 remained with no change, phosphorylation of RSK1 was seen 4 hours after the treatment. Levels of p-RSK1 continued to increase thereafter but declined at 24 hours (Figure 3A). Knockdown of RSK1 using two independent siRNAs drastically suppresses the induction of p-RSK1 by ADI (Figure 3B). Furthermore, we found that BI-D1870, which is a dihydropteridinone cell-permeable highly selective inhibitor of RSK family [45], exhibits a concentration-dependent inhibition of ADI induction of p-RSK1, p-EphA2(S897), and EphA2 expression. These findings suggest that RSK1 is responsible for ligand-independent EphA2(S879) activation by ADI. Phosphorylation of EphA2(S897) is induced via the PI3-kinase (PI3K)/MET/EKT-dependent mechanism (Figure 3C) [46]. Figure 3D shows that PI 103 (2 μM), a potent PI3K inhibitor, drastically inhibits ADI-induced p-RSK1, EphA2, and EphA2(S897) expression and that another PI3K inhibitor

Ly294002 (20 μM) moderately inhibits their expression (Figure 3E). Interestingly, we also found that perifosine, a potent AKT inhibitor [19], only marginally suppresses ADI-induced pRSK and EphA2 levels at high concentrations (10 μM) but enhances p-EphA2(S897) expression levels (Figure 3F). These results suggest that AKT, which is a downstream signal of PI3K, plays a negative role in ADI-induced p-EphA2(S897) activation. In other words, AKT plays an opposite role in regulating between Axl and EphA2 signaling.

Suppression of Axl Enhances ADI Induction of RSK1-EphA2 Signal

The observations that both Axl and Eph2 are activated by Arg starvation strongly suggest that these two RTK signals may be interactive. To investigate this possibility, we first used a c-Myc–tagged dominant-negative Axl recombinant (DN-Axl-c-Myc, *i.e.* K558R in the kinase domain) to downregulate the Axl signal [20]. We found that expression of DN-Axl-c-Myc enhances p-RSK1, EphA2, and p-EphA2(S897) expression (Figure 4A). To substantiate this finding, we used a truncated form of human Axl known as soluble Axl (sAxl) which contains only the extracellular ligand–binding domains. sAxl functions as a “sponge” to neutralize Gas6 ligand [47]. We previously demonstrated that sAxl suppresses Axl signaling induced by ADI [20]. Here, we show that sAxl induces p-RSK1, EphA2, and p-EphA2 expression (Figure 4A). These combined results demonstrate that downregulation of Axl upregulates the RSK1-EphA2 axis.

We also performed similar experiments using two arbitrary ADI^R cell lines (58R3 and 58R4). Downregulation of Axl in 58R3 and 59R4 cell lines by Axl siRNA resulted in upregulation of p-RSK1, EphA2, and p-EphA2(S897) but not RSK1, p-EphA2(Y588), and Ephrin A1 (Figure 4C). These results may support the compensatory role of RSK1-EphA2 in ADI-induced Gas6-Axl signal.

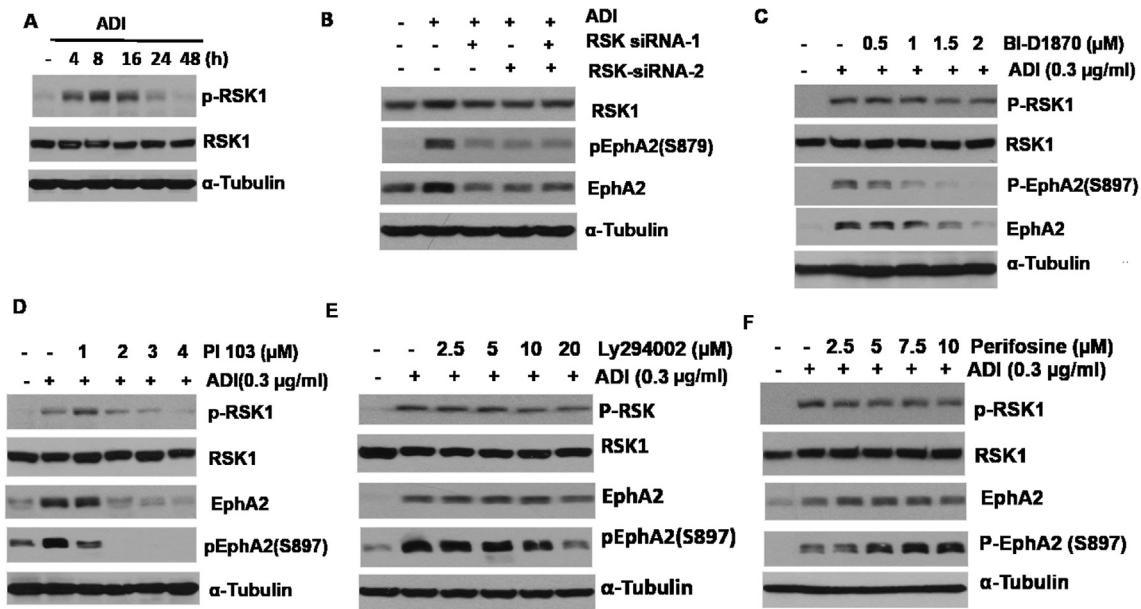


Figure 3. Activation of EphA2 by ADI is mediated by RSK1. (A) Time-dependent activation of p-RSK1 by ADI; (B) knockdown of RSK1 using two siRNAs shows suppression of EphA2 induction by ADI; (C) inhibition of EphA2 activation by RSK1 inhibitor BI-D1870; (D) and (E) inhibitions of ADI-induced activation of RSK1 and EphA2 by PI3K inhibitors PI-103 and Ly294002, respectively; (F) effects of AKT inhibitor (perifosine) on RSKs and EphA2 treated with ADI. (B–F) A2058 cells were treated with the indicated drugs for 24 hours. ADI, arginine deiminase.

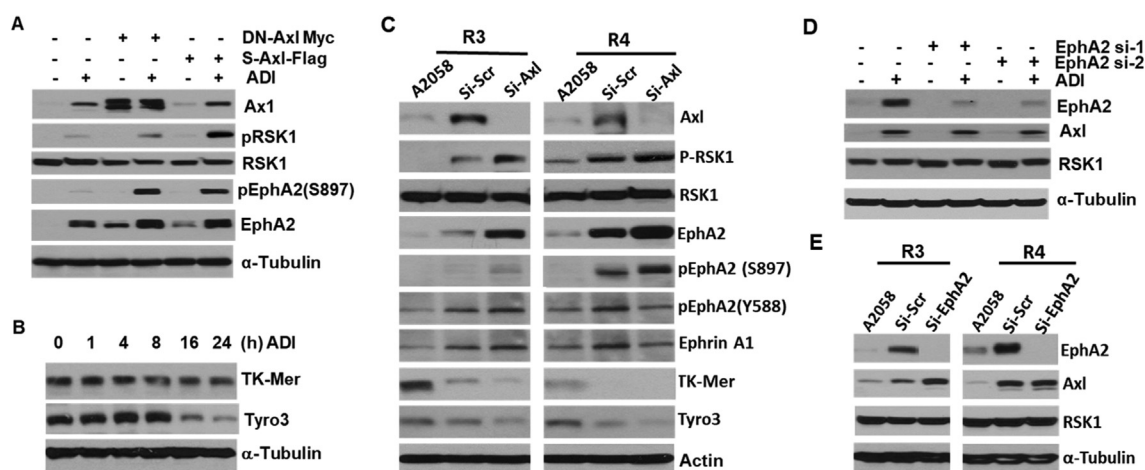


Figure 4. Interactions between Axl and EphA2 in response to ADI. (A) Inhibition of Axl activates RSK1 and EphA2 using dominant-negative (DN) Axl and soluble-Axl (s-Axl) recombinants in A2058 cells treated with ADI; (B) time-course suppression of TK-Mer and Tyro3 expression by ADI; (C) knockdown of Axl in two ADI^R (58R3 and 58R4) cells induces p-RSK1 and p-EphA2(S897) but downregulates TK-Mer and Tyro3, si-scr refers to scramble siRNA; (D) marginal regulation of Axl and RSK1 by EphA2 siRNA in A2058 cells; (E) Western blot assays showing that knockdown of EphA2 in two ADI^R cells moderately increase Axl expression.

Induction of ligand-dependent activation of Axl by ADI is initiated by externalization of Gas6, which is also the ligand of other TAM members, Tyro3 and Mer-TK. To investigate the behaviors of Tyro3 and Mer-TK in response to ADI, and specifically, whether enhanced RSK1-EphA2 under Axl-knockdown conditions may be mediated by Tyro3 or Mer-TK, we first determined the time-course expression of Tyro3 and Mer-TK in response to ADI treatment. We found that levels of Mer-TK were unchanged, whereas levels of Tyro3 were reduced after a 16-hours ADI treatment (Figure 4B). In addition, we found that knockdown of Axl reduced Tyro3 and TK-Mer expression in two ADI^R cell lines (Figure 4B). The opposite responses between Axl and Tyro3/TK-Mer to ADI challenge suggest that RSK1-EphA2 activation is likely independent of Tyro3/TK-Mer.

To investigate whether reduced EphA2 would have a reciprocal effect on Axl upregulation, we used two siRNAs to knockdown EphA2. We found that even greater than 90% reduction of EphA2 levels failed to affect ADI-induced Axl levels (Figure 4D). Moreover, knockdown of EphA2 by siRNA induces 2.5-fold and 55% increases of Axl expression in 58R3 and 58R4 ADI^R cells, respectively (Figure 4E). These results suggest that the RSK1-EphA2 signal does not reciprocally affect the expression of Axl in short-term ADI treatment, although long-term treatment results in increased Axl expression.

Elevated EphA2 Confers Acquired Resistance to EGFRi in ADI^R Cells

It would be of importance to investigate whether activation of EphA2/Axl in the ADI^R cells confers acquired resistance to RTK inhibitors. Figure 5A and Figure 5B show that all the 5 ADI^R cell lines exhibit resistance to lapatinib (Tykerb) and gefitinib, respectively, and levels of resistance ranging from 1.5-fold to > 2.5-fold. All the five ADI cell lines also show resistance to cetuximab (Erbix) at reduced levels (about 0.5-fold, P < 0.5) (data not shown). Both gefitinib and lapatinib inhibit EGFR signal by binding to the ATP-binding sites in their kinase domains [48,49], thereby preventing self-phosphorylation of the receptors and subsequent activation of their downstream signaling, whereas cetuximab is a

mouse/human chimeric monoclonal antibody that binds the extracellular ligand-binding domain of EGFR [50]. These observations suggest that the differential resistance to these EGFRi may be associated with different mechanisms of action of these inhibitors.

Knockdown of Axl failed to significantly increase cell killing activity of ADI^R cells to lapatinib (Figure 5C) but significantly increases sensitivity to the killing by gefitinib (Figure 5D). Importantly, knockdown of EphA2 increases sensitivity of both ADI^R cell lines to the killing to both lapatinib (Figure 5E) and gefitinib (Figure 5F). These results suggest that elevated EphA2 and, to a less extent, Axl are associated with acquired resistance of ADI^R cells to EGFR inhibitors.

Axl and EphA2 in ADI^R Cells are Regulated By c-Myc, and ADI^R Cells are Sensitive to c-Myc Inhibitor

We previously demonstrated that knockdown of c-Myc downregulates Axl [20]. Here, we found that knockdown of c-Myc also downregulates EphA2 expression in 58R3 and 58R4 cells (Figure 6A), indicating that EphA2 is also regulated by c-Myc. Moreover, we found that knockdown of c-Myc in 58R3 and 58R4 cells increased their sensitivities to lapatinib (Figure 6B) and gefitinib killing (Figure 6C). We also observed that coadministration of ADI and JQ1, a BET bromodomain-targeting c-Myc inhibitor [51], significantly increased cell killing of 58R3 (Figure 6C) and 58R4 cells by ADI (Figure 6D). These results demonstrate that anti-c-Myc drug can enhance ADI's cell killing activities.

Discussion

Long-term exposure of Arg-auxotrophic cells to Arg-free conditions results in the development of resistance to Arg-depleting agents such as ADI. While these ADI^R cells no longer require environmental Arg for survival, they however develop exquisite nutritional dependence for survival, as tested in charcoal-stripped FBS culture conditions. We observed that in many independently established ADI^R cell lines, several major RTKs (Axl, EphA2, and Met) are consistently overexpressed, and others (EGFR, Her2, and IGF1R) are sporadically overexpressed. We reason that upregulation of these RTKs is the consequence of protracted nutritional stress under ADI treatment.

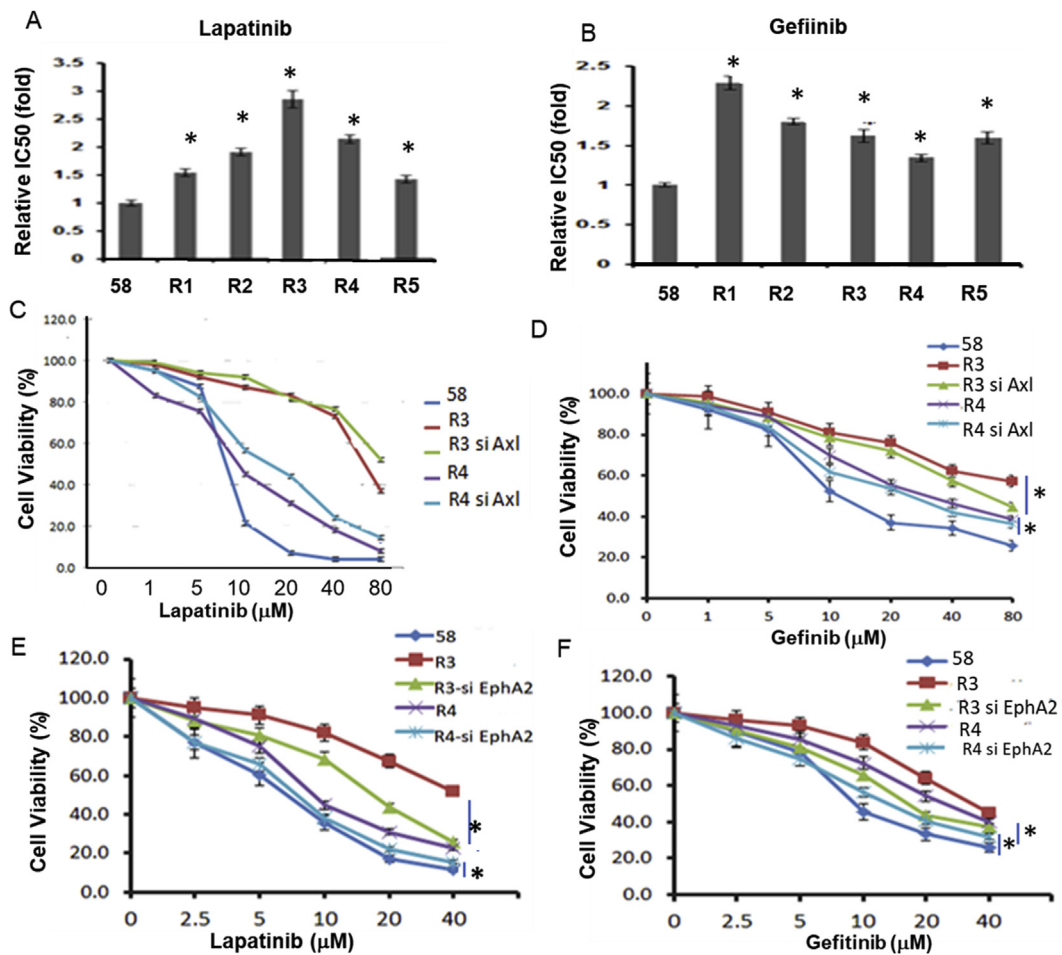


Figure 5. Effects of Axl and EphA2 knockdown by siRNAs on sensitivities of ADI^R cells to EGFRi. (A) and (B) Cell killing assays of five ADI^R cell lines treated with lapatinib or gefitinib as indicated; (C) and (D) effects of cell sensitivities to lapatinib or gefitinib, respectively, by Axl-knockdown, respectively; (E) and (F) effects of cell sensitivities to lapatinib or gefitinib, respectively, by EphA2-knockdown cells in ADI^R 58R3 and 58R4 cells. * denotes significant ($P < 0.05$).

These results document that surviving under long-term single amino acid deprivation such as Arg can enlist multiple RTKs requirements in cultured cells.

We have shown previously that ADI^R cells overexpress Axl [20]. In this report, we found that EphA2 expression is also induced in ADI^R cells. Importantly, we have elucidated the mechanisms underlying EphA2 activation by ADI and how it interacts with Axl as schematically depicted in Figure 7. Several important findings are described: First, we found that while PI3K-MEK-AKT is the ADI-induced Axl downstream pathway, this signal is also involved in ADI-induced EphA2 activation because PI3K inhibitors can suppress EphA2 activation. However, AKT apparently is not involved in EphA2 activation because AKT inhibitor (perifosine) fails to suppress EphA2 signal. Rather, we found that EphA2 activation is mediated by RSK1. ADI activates RSK1 by phosphorylation, which in turn activates pEphA2 (S897) by phosphorylation in a ligand-independent mechanism (Figure 7). Consistent with this notion, we found that the ligand-dependent pEphA2(Y588) is reduced. Nonetheless, despite many previous reports showing that elevated EphA2 is frequently associated with loss of Ephrin A1 ligand [52–54], no significant alteration of Ephrin A1 levels was found in ADI-treated cells and in ADI^R cells. Thus, ADI-induced activation of RTKs can be either ligand-dependent or ligand-independent (Figure 7).

Second, we found that knockdown of Axl upregulates EphA2 via RSK1 activation in both ADI-treated and in ADI^R cells, suggesting that EphA2 is functionally compensatory of Axl. In contrast, knockdown of EphA2 only marginally increases Axl levels, suggesting that Axl plays less compensatory role than EphA2 does in Arg-starvation challenge. Many recent studies have demonstrated that activated Axl cross-activated other RTKs including EGFR, Met, and PDGF; and Axl can form heterodimer with EGFR [55–58]. However, we found no corresponding increases of EGFR among 5 ADI^R lines investigated. Moreover, the unsymmetrical cross-talk between Axl and EphA2 signalings described here has not been reported.

Third, in addition to RSK1, we found that EphA2 is regulated by c-Myc. Whether c-Myc transcriptionally regulates EphA2 remains to be firmly established although we found that several c-Myc-binding sites are located at the promoter of *EphA2*. These findings, together with our previous demonstrations that c-Myc transcriptionally regulates *ASS1* [19] and *Axl* [20], underscore the importance of c-Myc in overall Arg homeostasis regulation (Figure 7). In a broad context, recent studies have established that deregulation of c-Myc is associated with many human malignancies. Many c-Myc-driven cancers are characterized by altered metabolism including heightened nutrient requirement, enhanced glycolysis, and glutaminolysis [59].

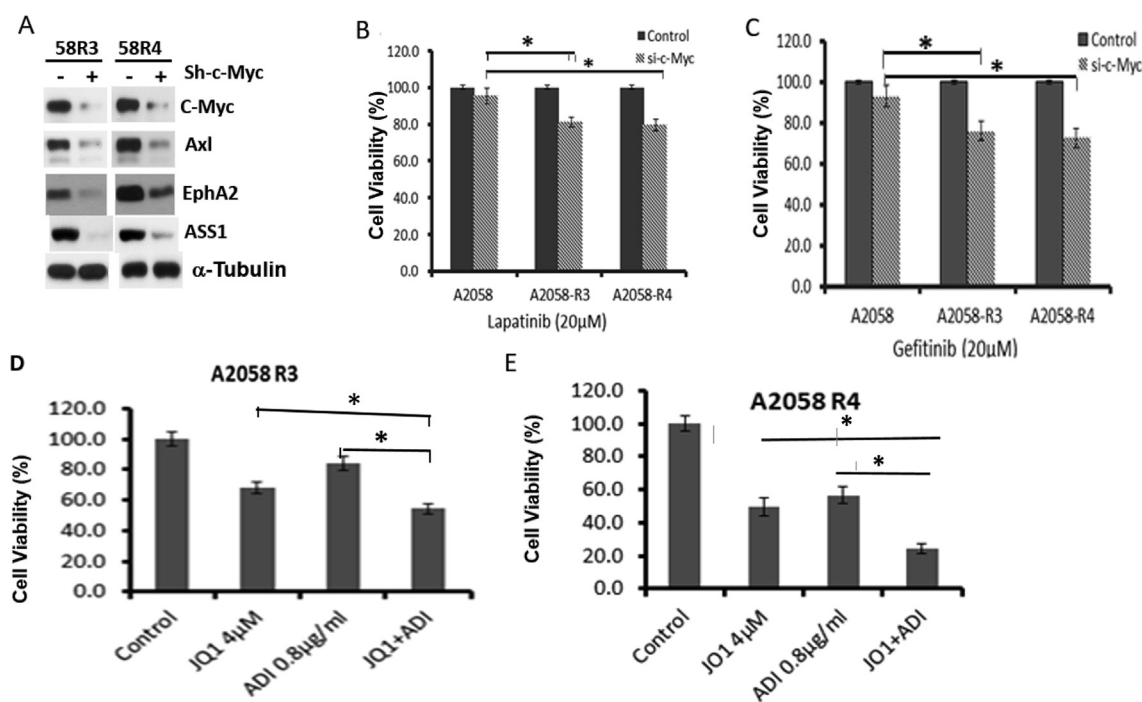


Figure 6. Effects of c-Myc knockdown on the growth of ADI^R (58R3 and 58R4) cells to EGFRi. (A) Western blots showing reduced expression of Axl, EphA2, and ASS1 in two ADI^R cells; (B) and (C) effects of c-Myc knockdown on cell proliferation of A2058 and ADI^R treated with lapatinib and gefitinib, respectively; (D) and (E) increases of cell killing effects by JQ1 in combination therapy with ADI on 58R3 and 58R4, respectively.

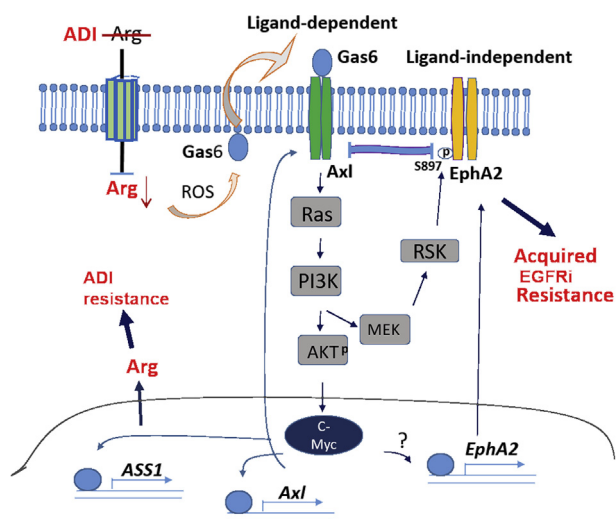


Figure 7. Schematic diagram depicting Axl and EphA2 signaling to Arg starvation response in Arg auxotrophic cells. Arg depletion using ADI induces ligand (Gas)-dependent activation of Axl and its downstream signal leading to induced c-Myc expression described previously [20] and ligand-independent activation of EphA2 via the PI3K-MEK-RSK axis. c-Myc transcriptionally induces ASS1 expression resulting in arginine synthesis and hence ADI resistance. c-Myc also transcriptionally regulates Axl to amplify the Axl-PI3K-AKT loop. c-Myc upregulates EphA2 expression (perhaps by transcriptional mechanism as denoted by “?”), leading to acquired resistance to EGFRi. Horizontal bar denotes interaction between Axl and EphA2. ADI, arginine deiminase.

Our observations that ADI^R variants are preferentially sensitive to charcoal-stripped FBS cultured conditions described here, and are addict to glucose and glutamine for growth previously published [30], may at least in part be attributed to the altered c-Myc expression in these cells. These findings suggest that c-Myc may be an important target for augmenting the therapeutic effect of Arg starvation therapy. As a proof of principle, we found that c-Myc inhibitor JQ1 can enhance ADI's cell killing capacities of ADI^R cells. We note that, in contrast, c-Myc apparently does not regulate Met which is also frequently upregulated in ADI^R cells (data not shown).

Fourth, we discover that ADI^R cells exhibit resistance to EGFRi. We reason that this acquired resistance is attributed to the upregulated EphA2 and, to a less extent, Axl knockdown of these RTKs sensitizes these cells to EGFRi. Overexpression of Axl has been reported to associate with reduced sensitivity to EGFRi in cetuximab-resistant non-small cell lung cancer [60] and head and neck cancer [61]. Furthermore, Rho et al. [62] have also reported antitumor activity of AXL inhibitor in EGFRi-resistant lung cancer cells. Similarly, elevated EphA2 levels have been reported to associate with resistance to EGFRi trastuzumab. Many small molecular inhibitors for Axl have been in various stages of clinical evaluations [63,64]; these inhibitors have also shown cross-inhibition of other RTKs with reduced efficacies. EphA2 is frequently upregulated in EGFR-overexpressing cancer cell lines, and targeting these resistant variants with EphA2 inhibition can reduce tumor cell proliferation and increase apoptosis [65]. Our results show that while some RTK inhibitors such as foretinib may be beneficial for combination therapy with ADI, others such as EGFRi [66,67] may not be effective in targeted therapy against Arg-auxotrophic tumors.

In conclusion, we have demonstrated the multifacets of RTK in Arg starvation response and that selective RTK inhibitors may be of value for developing strategies of overcoming ADI resistance. Our current findings provide a mechanistic base for clinical investigations that may ultimately improve the treatment outcomes of targeting Arg-auxotrophic therapy in cancers.

Acknowledgments

The authors thank Drs. Bor-Wen Wu and John Bomalaski (Polaris Pharmaceuticals, Inc) for ADI-PEG20 and anti-ASS1 antibody. This work was supported in part by grants from the National Cancer Institute (R01 CA149260 to MTK, NS and LGF), VA merit award (1101BX003328-01 to NS), and Ministry of Science and Technology, Taiwan (MOST-105-2314-B-006-046-My3 to HHWC).

Appendix A. Supplementary data

Supplementary data to this article can be found online at <https://doi.org/10.1016/j.tranon.2019.12.003>.

References

- Closs EI, Simon A, Vekony N and Rotmann A (2004). Plasma membrane transporters for arginine. *J Nutr* **134**, 2752S–2759S. discussion 2765S–2767S.
- Dillon BJ, Prieto VG, Curley SA, Ensor CM, Holtsberg FW, Bomalaski JS and Clark MA (2004). Incidence and distribution of argininosuccinate synthetase deficiency in human cancers: a method for identifying cancers sensitive to arginine deprivation. *Cancer* **100**, 826–833.
- Mussai F, Egan S, Higginbotham-Jones J, Perry T, Beggs A, Odintsova E, Loke J, Pratt G, U KP and Lo A, et al (2015). Arginine dependence of acute myeloid leukemia blast proliferation: a novel therapeutic target. *Blood* **125**, 2386–2396.
- Kuo MT, Savaraj N and Feun LG (2010). Targeted cellular metabolism for cancer chemotherapy with recombinant arginine-degrading enzymes. *Oncotarget* **1**, 246–251.
- Savaraj N, You M, Wu C, Wangpaichitr M, Kuo MT and Feun LG (2010). Arginine deprivation, autophagy, apoptosis (AAA) for the treatment of melanoma. *Curr Mol Med* **10**, 405–412.
- Tsai HJ, Jiang SS, Hung WC, Borthakur G, Lin SF, Pemmaraju N, Jabbour E, Bomalaski JS, Chen YP and Hsiao HH, et al (2017). A phase II study of arginine deiminase (ADI-PEG20) in relapsed/refractory or poor-risk acute myeloid leukemia patients. *Sci Rep* **7**, 11253.
- Lowery MA, Yu KH, Kelsen DP, Harding JJ, Bomalaski JS, Glassman DC, Covington CM, Brenner R, Hollywood E and Barba A, et al (2017). A phase 1/1B trial of ADI-PEG 20 plus nab-paclitaxel and gemcitabine in patients with advanced pancreatic adenocarcinoma. *Cancer* **123**, 4556–4565.
- Thongkum A, Wu C, Li YY, Wangpaichitr M, Navasumrit P, Parnlob V, Sricharunrat T, Bhudhisawasdi V, Ruchirawat M and Savaraj N (2017). The combination of arginine deprivation and 5-fluorouracil improves therapeutic efficacy in argininosuccinate synthetase negative hepatocellular carcinoma. *Int J Mol Sci* **18**.
- Beddowes E, Spicer J, Chan PY, Khadeir R, Corbacho JG, Repana D, Steele JP, Schmid P, Szyszko T and Cook G, et al (2017). Phase 1 dose-escalation study of pegylated arginine deiminase, cisplatin, and pemetrexed in patients with argininosuccinate synthetase 1-deficient thoracic cancers. *J Clin Oncol* **35**, 1778–1785.
- Szlosarek PW, Steele JP, Nolan L, Gilligan D, Taylor P, Spicer J, Lind M, Mitra S, Shamash J and Phillips MM, et al (2017). Arginine deprivation with pegylated arginine deiminase in patients with argininosuccinate synthetase 1-deficient malignant pleural mesothelioma: A Randomized Clinical Trial. *JAMA Oncol* **3**, 58–66.
- Savaraj N, Wu C, Li YY, Wangpaichitr M, You M, Bomalaski J, He W, Kuo MT and Feun LG (2015). Targeting argininosuccinate synthetase negative melanomas using combination of arginine degrading enzyme and cisplatin. *Oncotarget* **6**, 6295–6309.
- Tomlinson BK, Thomson JA, Bomalaski JS, Diaz M, Akande T, Mahaffey N, Li T, Dutia MP, Kelly K and Gong IY, et al (2015). Phase I trial of arginine deprivation therapy with ADI-PEG 20 plus docetaxel in patients with advanced malignant solid tumors. *Clin Cancer Res* **21**, 2480–2486.
- De Santo C, Booth S, Vardon A, Cousins A, Tubb V, Perry T, Noyvert B, Beggs A, Ng M and Halsey C, et al (2018). The arginine metabolome in acute lymphoblastic leukemia can be targeted by the pegylated-recombinant arginase I BCT-100. *Int J Cancer* **142**, 1490–1502.
- Yau T, Cheng PN, Chan P, Chen L, Yuen J, Pang R, Fan ST, Wheatley DN and Poon RT (2015). Preliminary efficacy, safety, pharmacokinetics, pharmacodynamics and quality of life study of pegylated recombinant human arginase I in patients with advanced hepatocellular carcinoma. *Investig New Drugs* **33**, 496–504.
- Ott PA, Carvajal RD, Pandit-Taskar N, Jungbluth AA, Hoffman EW, Wu BW, Bomalaski JS, Venhaus R, Pan L and Old LJ, et al (2013). Phase I/II study of pegylated arginine deiminase (ADI-PEG 20) in patients with advanced melanoma. *Investig New Drugs* **31**, 425–434.
- Tsai WB, Aiba I, Lee SY, Feun L, Savaraj N and Kuo MT (2009). Resistance to arginine deiminase treatment in melanoma cells is associated with induced argininosuccinate synthetase expression involving c-Myc/HIF-1alpha/Sp4. *Mol Cancer Ther* **8**, 3223–3233.
- Szlosarek PW, Klabatsa A, Pallaska A, Sheaff M, Smith P, Crook T, Grimshaw MJ, Steele JP, Rudd RM and Balkwill FR, et al (2006). In vivo loss of expression of argininosuccinate synthetase in malignant pleural mesothelioma is a biomarker for susceptibility to arginine depletion. *Clin Cancer Res* **12**, 7126–7131.
- Tsai WB, Long Y, Chang JT, Savaraj N, Feun LG, Jung M, Chen HHW and Kuo MT (2017). Chromatin remodeling system p300-HDAC2-Sin3A is involved in Arginine Starvation-Induced HIF-1alpha Degradation at the ASS1 promoter for ASS1 Derepression. *Sci Rep* **7**, 10814.
- Tsai WB, Aiba I, Long Y, Lin HK, Feun L, Savaraj N and Kuo MT (2012). Activation of Ras/PI3K/ERK pathway induces c-Myc stabilization to upregulate argininosuccinate synthetase, leading to arginine deiminase resistance in melanoma cells. *Cancer Res* **72**, 2622–2633.
- Tsai WB, Long Y, Park JR, Chang JT, Liu H, Rodriguez-Canales J, Savaraj N, Feun LG, Davies MA and Wistuba II, et al (2016). Gas6/Axl is the sensor of arginine-auxotrophic response in targeted chemotherapy with arginine-depleting agents. *Oncogene* **35**, 1632–1642.
- Lemke G (2013). Biology of the TAM receptors. *Cold Spring Harbor Perspect Biol* **5**. a009076.
- Graham DK, DeRyckere D, Davies KD and Earp HS (2014). The TAM family: phosphatidylinositol sensing receptor tyrosine kinases gone awry in cancer. *Nat Rev Cancer* **14**, 769–785.
- Verma A, Warner SL, Vankayalapati H, Bearss DJ and Sharma S (2011). Targeting Axl and mer kinases in cancer. *Mol Cancer Ther* **10**, 1763–1773.
- Vouri M and Hafizi S (2017). TAM receptor tyrosine kinases in cancer Drug Resistance. *Cancer Res* **77**, 2775–2778.
- Antony J and Huang RY (2017). AXL-driven EMT state as a targetable conduit in cancer. *Cancer Res* **77**, 3725–3732.
- Wu F, Li J, Jang C, Wang J and Xiong J (2014). The role of Axl in drug resistance and epithelial-to-mesenchymal transition of non-small cell lung carcinoma. *Int J Clin Exp Pathol* **7**, 6653–6661.
- Byers LA, Diao L, Wang J, Saintigny P, Girard L, Peyton M, Shen L, Fan Y, Giri U and Tumula PK, et al (2013). An epithelial-mesenchymal transition gene signature predicts resistance to EGFR and PI3K inhibitors and identifies Axl as a therapeutic target for overcoming EGFR inhibitor resistance. *Clin Cancer Res* **19**, 279–290.
- Asiedu MK, Beauchamp-Perez FD, Ingle JN, Behrens MD, Radisky DC and Knutson KL (2014). AXL induces epithelial-to-mesenchymal transition and regulates the function of breast cancer stem cells. *Oncogene* **33**, 1316–1324.
- De Craene B and Bex G (2013). Regulatory networks defining EMT during cancer initiation and progression. *Nat Rev Cancer* **13**, 97–110.
- Long Y, Tsai WB, Wangpaichitr M, Tsukamoto T, Savaraj N, Feun LG and Kuo MT (2013). Arginine deiminase resistance in melanoma cells is associated with metabolic reprogramming, glucose dependence, and glutamine addiction. *Mol Cancer Ther* **12**, 2581–2590.
- Du Z and Lovly CM (2018). Mechanisms of receptor tyrosine kinase activation in cancer. *Mol Cancer* **17**, 58.

- [32] Schlessinger J (2014). Receptor tyrosine kinases: legacy of the first two decades. *Cold Spring Harbor Perspect Biol* **6**.
- [33] Lemmon MA and Schlessinger J (2010). Cell signaling by receptor tyrosine kinases. *Cell* **141**, 1117–1134.
- [34] Zhang J, Pavlova NN and Thompson CB (2017). Cancer cell metabolism: the essential role of the nonessential amino acid, glutamine. *EMBO J* **36**, 1302–1315.
- [35] Henry CM, Hollville E and Martin SJ (2013). Measuring apoptosis by microscopy and flow cytometry. *Methods* **61**, 90–97.
- [36] Orellana EA and Kasinski AL (2016). Sulforhodamine B (SRB) assay in cell culture to investigate cell proliferation. *Bio Protoc* **6**.
- [37] Cantor JR, Abu-Remaileh M, Kanarek N, Freinkman E, Gao X, Louissaint Jr A, Lewis CA and Sabatini DM (2017). Physiologic medium rewires cellular metabolism and reveals uric acid as an endogenous inhibitor of UMP Synthase. *Cell* **169**, 258–272 e217.
- [38] Manning BD and Cantley LC (2007). AKT/PKB signaling: navigating downstream. *Cell* **129**, 1261–1274.
- [39] Yau TCC, Lencioni R, Sukeepaisarnjaroen W, Chao Y, Yen CJ, Lausontornsiri W, Chen PJ, Sanpajit T, Camp A and Cox DS, et al (2017). A phase I/II multicenter study of single-agent foretinib as first-line therapy in patients with advanced hepatocellular carcinoma. *Clin Cancer Res* **23**, 2405–2413.
- [40] Wiedemann E, Jellinghaus S, Ende G, Augstein A, Sczech R, Wielockx B, Weinert S, Strasser RH and Poitz DM (2017). Regulation of endothelial migration and proliferation by ephrin-A1. *Cell Signal* **29**, 84–95.
- [41] Zhou Y and Sakurai H (2017). Emerging and diverse functions of the EphA2 noncanonical pathway in cancer progression. *Biol Pharm Bull* **40**, 1616–1624.
- [42] Hamaoka Y, Negishi M and Katoh H (2016). EphA2 is a key effector of the MEK/ERK/RSK pathway regulating glioblastoma cell proliferation. *Cell Signal* **28**, 937–945.
- [43] Houles T and Roux PP (2018). Defining the role of the RSK isoforms in cancer. *Semin Cancer Biol* **48**, 53–61.
- [44] Romeo Y, Zhang X and Roux PP (2012). Regulation and function of the RSK family of protein kinases. *Biochem J* **441**, 553–569.
- [45] Sapkota GP, Cummings L, Newell FS, Armstrong C, Bain J, Frodin M, Grauert M, Hoffmann M, Schnapp G and Steegmaier M, et al (2007). BI-D1870 is a specific inhibitor of the p90 RSK (ribosomal S6 kinase) isoforms in vitro and in vivo. *Biochem J* **401**, 29–38.
- [46] Harada K, Negishi M and Katoh H (2015). HGF-induced serine 897 phosphorylation of EphA2 regulates epithelial morphogenesis of MDCK cells in 3D culture. *J Cell Sci* **128**, 1912–1921.
- [47] Ekman C, Stenhoff J and Dahlback B (2010). Gas6 is complexed to the soluble tyrosine kinase receptor Axl in human blood. *J Thromb Haemost* **8**, 838–844.
- [48] Pao W, Miller V, Zakowski M, Doherty J, Politi K, Sarkaria I, Singh B, Heelan R, Rusch V and Fulton L, et al (2004). EGF receptor gene mutations are common in lung cancers from "never smokers" and are associated with sensitivity of tumors to gefitinib and erlotinib. *Proc Natl Acad Sci U S A* **101**, 13306–13311.
- [49] Burns-Hamuro LL, Barraclough DM and Taylor SS (2004). Identification and functional analysis of dual-specific A kinase-anchoring protein-2. *Methods Enzymol* **390**, 354–374.
- [50] Lenz HJ (2006). Anti-EGFR mechanism of action: antitumor effect and underlying cause of adverse events. *Oncology (Williston Park)* **20**, 5–13.
- [51] Delmore JE, Issa GC, Lemieux ME, Rahl PB, Shi J, Jacobs HM, Kastiris E, Gilpatrick T, Paranal RM and Qi J, et al (2011). BET bromodomain inhibition as a therapeutic strategy to target c-Myc. *Cell* **146**, 904–917.
- [52] Dodelet VC and Pasquale EB (2000). Eph receptors and ephrin ligands: embryogenesis to tumorigenesis. *Oncogene* **19**, 5614–5619.
- [53] Pasquale EB (2008). Eph-ephrin bidirectional signaling in physiology and disease. *Cell* **133**, 38–52.
- [54] Wykosky J, Gibo DM, Stanton C and Debinski W (2005). EphA2 as a novel molecular marker and target in glioblastoma multiforme. *Mol Cancer Res* **3**, 541–551.
- [55] Antony J, Tan TZ, Kelly Z, Low J, Choolani M, Recchi C, Gabra H, Thiery JP and Huang RY (2016). The GAS6-AXL signaling network is a mesenchymal (Mes) molecular subtype-specific therapeutic target for ovarian cancer. *Sci Signal* **9**, ra97.
- [56] Meyer AS, Miller MA, Gertler FB and Lauffenburger DA (2013). The receptor AXL diversifies EGFR signaling and limits the response to EGFR-targeted inhibitors in triple-negative breast cancer cells. *Sci Signal* **6**, ra66.
- [57] Vouri M, Croucher DR, Kennedy SP, An Q, Pilkington GJ and Hafizi S (2016). Axl-EGFR receptor tyrosine kinase hetero-interaction provides EGFR with access to pro-invasive signalling in cancer cells. *Oncogenesis* **5**, e266.
- [58] Elkabets M, Pazarentzos E, Juric D, Sheng Q, Pelosof RA, Brook S, Benzaken AO, Rodon J, Morse N and Yan JJ, et al (2015). AXL mediates resistance to PI3Kalpha inhibition by activating the EGFR/PKC/mTOR axis in head and neck and esophageal squamous cell carcinomas. *Cancer Cell* **27**, 533–546.
- [59] Hsieh AL, Walton ZE, Altman BJ, Stine ZE and Dang CV (2015). MYC and metabolism on the path to cancer. *Semin Cell Dev Biol* **43**, 11–21.
- [60] Brand TM, Iida M, Stein AP, Corrigan KL, Braverman CM, Luthar N, Toulany M, Gill PS, Salgia R and Kimple RJ, et al (2014). AXL mediates resistance to cetuximab therapy. *Cancer Res* **74**, 5152–5164.
- [61] Giles KM, Kalinowski FC, Candy PA, Epis MR, Zhang PM, Redfern AD, Stuart LM, Goodall GJ and Leedman PJ (2013). Axl mediates acquired resistance of head and neck cancer cells to the epidermal growth factor receptor inhibitor erlotinib. *Mol Cancer Ther* **12**, 2541–2558.
- [62] Rho JK, Choi YJ, Kim SY, Kim TW, Choi EK, Yoon SJ, Park BM, Park E, Bae JH and Choi CM, et al (2014). MET and AXL inhibitor NPS-1034 exerts efficacy against lung cancer cells resistant to EGFR kinase inhibitors because of MET or AXL activation. *Cancer Res* **74**, 253–262.
- [63] Wu X, Liu X, Koul S, Lee CY, Zhang Z and Halmos B (2014). AXL kinase as a novel target for cancer therapy. *Oncotarget* **5**, 9546–9563.
- [64] Feneuyrolles C, Spelinshauer A, Guet L, Fauvel B, Dayde-Cazals B, Warnault P, Cheve G and Yasri A (2014). Axl kinase as a key target for oncology: focus on small molecule inhibitors. *Mol Cancer Ther* **13**, 2141–2148.
- [65] Amato KR, Wang S, Tan L, Hastings AK, Song W, Lovly CM, Meador CB, Ye F, Lu P and Balko JM, et al (2016). EPHA2 blockade overcomes acquired resistance to EGFR kinase inhibitors in lung cancer. *Cancer Res* **76**, 305–318.
- [66] Mountzios G (2018). Making progress in epidermal growth factor receptor (EGFR)-mutant non-small cell lung cancer by surpassing resistance: third-generation EGFR tyrosine kinase inhibitors (EGFR-TKIs). *Ann Transl Med* **6**, 140.
- [67] Hsu WH, Yang JC, Mok TS and Loong HH (2018). Overview of current systemic management of EGFR-mutant NSCLC. *Ann Oncol* **29**, i3–i9.